RP Current Trends In Engineering And Technology (e-ISSN: 2583-5491)
Vol. 5, No. 3 (July – September 2026) pp. 69–76

RESEARCH PLATEAU PUBLISHERS

Cite this article: R. Deshmukh, N. Hande, P. Mattikalli, C. Bhanarkar, M.K. Bhanarkar, Validation of compact multiband meandered shape antenna, *RP Cur. Tr. Eng. Tech.* **5** (2026) 69–76.

Original Research Article

Validation of compact multiband meandered shape antenna

Ratnadeep Deshmukh[1,*], Nirmala Hande[1], Paresh Mattikalli[1], Charushila Bhanarkar[2], M.K. Bhanarkar[1]

[1]Antenna Design Laboratory, Department of Electronics, Shivaji University, Kolhapur, India
[2]Gopal Krishna Gokhale College, Kolhapur, India
*Corresponding author, E-mail: rd4ratnadeep@gmail.com

ARTICLE HISTORY
Received: 19 April 2026
Revised: 03 July 2026
Accepted: 04 July 2026
Published: 06 July 2026

KEYWORDS
Compact; Wideband; Multiband; Microstrip antenna; Meander.

ABSTRACT
Antenna has numerous important in wireless communication system for 5G as well as 6G. In this research paper, the design and fabrication of a compact multiband meandered microstrip antenna results are carried out which is implemented with FR4 substrate. The antenna employs symmetric meander line geometry to achieve multiple resonant modes across a wide frequency range while maintaining a compact physical footprint. Full wave electromagnetic simulation predicts six resonant frequencies between 1 and 10 GHz. Measured resonances occur at approximately 1.81, 2.62, 5.32, 6.08, 7.08, 8.24, 9.28 GHz, showing reasonable agreement with simulated results. The antenna exhibits 10 dB impedance and 7.5 GHz bandwidth. A comparative analysis with recently published multiband antennas demonstrates favorable performance in terms of bands, dimensions and structure. The proposed antenna is applicable for WLAN, LTE, sub-6 GHz, 5G applications.

1. Introduction

Compact multiband antennas are essential to modern wireless systems, since handheld, embedded, and IoT platforms increasingly require the capability to provide many services within a single low-profile radiator. Micro-strip antennas are appealing due to their planar design, ease of integration, and compatibility with printed circuit manufacturing; nonetheless, their traditional configurations are often narrowband and tend to accommodate a limited number of resonant modes [1], [2]. To address these limitations, previous research has investigated slot loading, fractal shaping, parasitic stubs, metamaterial loading, defective ground structures, and meandering current paths [3], [4]. Among these solutions, meander geometries are particularly advantageous for miniaturization, as they extend the effective surface current pathway while maintaining a compact physical footprint. The primary problem is that significant miniaturization frequently compromises realized gain, radiation efficiency, and impedance stability, particularly when employing low-cost FR4 substrate.

The constructed prototype maintains multi-resonant characteristics throughout an extensive frequency range of 1-10 GHz and exhibits a broad operational window with several distinct resonances. Integrating the simulated and empirical evidence into a unified analytical discourse; implementing a more stringent analysis of the deviation between simulation and measurement; assessing the radiation efficiency detriment linked to the compact FR4 meander design; consequently, the practical contribution of this work extends beyond the radiator configuration itself, providing a more lucid experimental validation of how a structurally simplified meander can produce multiple advantageous resonances across an extensive frequency range.

2. Related literature and research gap

Recent literature indicates various approaches to achieving compact multiband performance. Ali et al. introduced a miniaturized multiband antenna, followed by a fractal quad-band antenna incorporating an L-shaped slot and metamaterials, illustrating how distributed slotting and artificial loading can generate multiple resonant pathways [5], [6]. Khan et al. documented a compact four-band slot antenna with dimensions of 20 × 20 × 1.6 mm^3, demonstrating that diminutive substrates can effectively facilitate multiband functionality when slot resonators are appropriately linked [7]. Patel et al. presented a low-profile meander antenna on FR4 for LTE/WiMAX/WLAN/INSAT-C applications and later expanded this methodology in their study on Wireless Networks, both of which emphasizes the significance of meander-inspired current regulation in practical wireless systems [8], [9]. Abolade and Konditi integrated a small meander with a shorting pin to achieve six resonances in a portable platform [10]. Recent studies by Maamria et al., Islam et al., and Lin et al. further substantiate that compact multiband operation can be attained via meandered parasitics, multi-stub loading, and coupling control features, albeit with varying trade-offs in size, application bandwidth, gain, efficiency, and fabrication complexity [11], [12].

The research gap identified is specific: numerous published antennas attain a restricted number of discrete bands, possess a bigger footprint, or exhibit a geometry that complicates fabrication and reproduction using ordinary FR4 prototyping. The current antenna seeks to preserve geometric simplicity while producing a somewhat dense multi-resonant response and ensuring satisfactory impedance matching post-fabrication.

3. Antenna configuration and design consideration

The suggested antenna is fabricated on a FR4 substrate with a relative permittivity of εr = 4.4 and a thickness of h = 1.6 mm. The radiator contains four mirrored meander arms interconnected around a central feed area and energized by a 50 Ω microstrip line. Symmetry was deliberately maintained to stabilize the current distribution and prevent an overly asymmetric radiation response. The meandered sections extend the electrical length of the current pathway, while the reduced space between arms facilitates capacitive coupling among neighboring segments. The synergistic inductive-capacitive effect generates several resonant modes within a small design. The suggested radiator employs a mirrored meander design to enhance the effective current pathway and to stimulate several resonant modes without enlarging the overall footprint.

3.1 Design consideration

The fundamental resonance of a straight micro-strip antenna of length L is

$$f_r = \frac{c}{2\, L_{eff}\sqrt{\varepsilon_{eff}}}$$

where,

$c = 3 \times 10^8$ ms^{-1},

f_r = Resonant frequency,

L_{eff} = Effective patch length,

ε_{eff} = Effective dielectric constant.

$$\varepsilon_{eff} = \frac{\varepsilon_r+1}{2} + \frac{\varepsilon_r-1}{2}\left(1 + 12\,\frac{h}{W_p}\right)^{0.5}$$

The meander arms extend the electrical length, so the effective resonant frequency becomes

$$L_{eff} = L_p + 2\Delta L$$

$$\Delta L = 0.412h\,\frac{(\varepsilon_{eff} + 0.3)\left(\frac{W}{L} + 0.264\right)}{(\varepsilon_{eff} - 0.258)\left(\frac{W}{L} + 0.8\right)}$$

$$Z_0 = \frac{60}{\sqrt{\varepsilon_{eff}}}\ln\left(\frac{8h}{W_f} + 0.25\right)(4\pi A_{eff}/\lambda^2).$$

3.2 Geometry of the proposed antenna

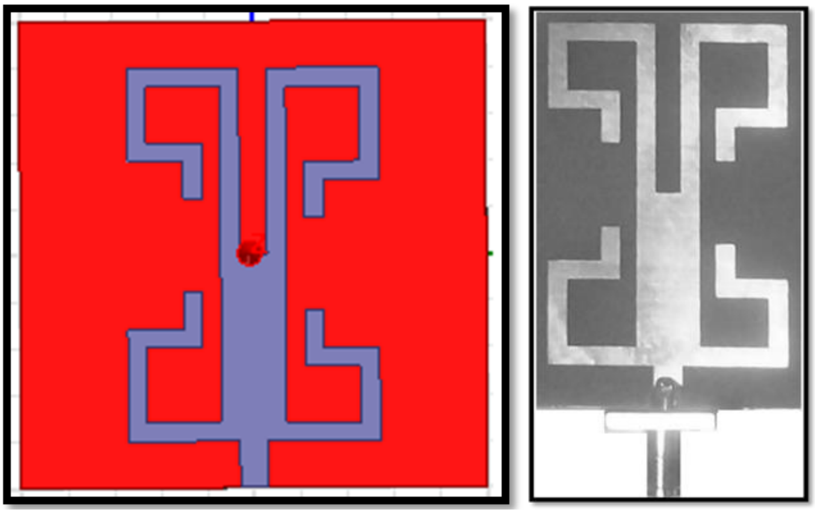

Figure 1: Simulated geometry (left) and fabricated prototype (right) of the proposed symmetric meandered antenna.

Figure 1 confirms that the structural simplicity of the proposed design. The radiator used four mirrored meandered arms around a centrally fed lower stem. The fabricated sample preserves the essential design of the simulation model, which is important because compact antennas are often highly sensitive to small layout impacts.

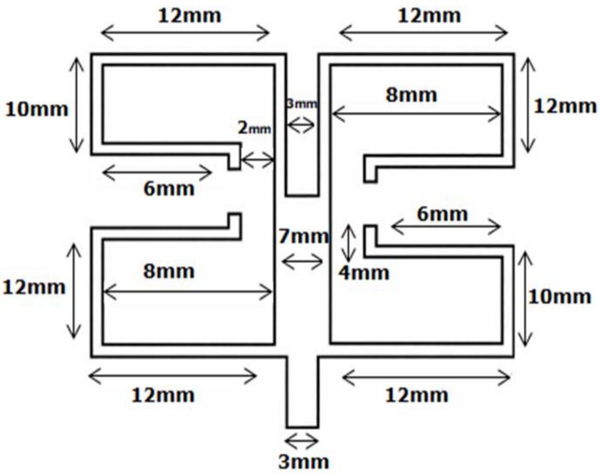

Figure 2: Optimized geometric dimensions of the proposed antenna.

Table1: Optimized dimensions of the proposed antenna.

Parameter	Description	Value (mm)
Substrate (LP × WP × *h*)	FR4 substrate dimensions	50 × 50 × 1.6
Ground plane (LG × WG)	Bottom ground dimensions	50 × 50
Feed (LF × WF)	50 Ω micro-strip feed	25 × 3
WM	Meander strip width	2
S	Arm spacing	2
Upper-left meander	Segment lengths L1–L4	12, 10, 6, 4
Upper-right meander	Segment lengths L1–L4	12, 12, 6, 4
Lower-right meander	Segment lengths L1–L4	12, 12, 6, 4
Lower-left meander	Segment lengths L1–L4	12, 10, 6, 4

3.3 Operating principle

For a conventional rectangular micro-strip radiator, a first order estimate of the dominant resonant frequency can be written as:

$$f_r \approx c / (2\, L_{eff} \sqrt{\varepsilon_{eff}})$$

$$\varepsilon_{eff} \approx (\varepsilon_r + 1)/2 + (\varepsilon_r - 1)/2 \cdot (1 + 12h/W)^{-1/2}$$

$$\Delta L/h \approx 0.412 \cdot [(\varepsilon_{eff} + 0.3)\,(W/h + 0.264)] / [(\varepsilon_{eff} - 0.258)\,(W/h + 0.8)]$$

In the present design, however, these closed form relations serve only as an initialization guide. The actual resonant frequencies are governed by the longer folded current path, inter-arm coupling and interaction with the ground plane, and were therefore finalized through full-wave optimization.

4. Simulation and experimental methodology

The antenna was modeled in ANSYS HFSS using a driven-modal solution setup, lumped-port excitation, adaptive meshing, and a 1–10 GHz frequency sweep. The use of a full-wave finite-element solver is appropriate here because the radiator contains tightly coupled narrow meander sections whose electromagnetic interactions are not accurately captured by simplified circuit models alone. In addition to reflection coefficient and VSWR, the solver was used to observe the two-dimensional radiation pattern, 3D realized gain, 3D directivity, and impedance matching on the Smith chart.

A prototype of the optimized design was fabricated by standard PCB etching on FR4 and fed through an SMA connector. The reflection coefficient and VSWR were measured using a calibrated vector network analyzer over 1–10 GHz. As expected for FR4-based compact antennas, differences between simulated and measured results can arise from dielectric-constant uncertainty, copper and dielectric losses, etching tolerance, connector parasitics, and solder-induced feed impacts.

5. Result and discussion

The accomplished antenna exhibits a distinct multi-resonant response in both simulation and experimentation. The computed S11 plot indicates six resonances below -10 dB, while the built prototype displays seven measured minima within the identical frequency range. The measured result is significant as the annotated return loss curve reveals a broad continuous -10 dB bandwidth of about 7.515 GHz, indicating that the manufactured antenna functions as both a multiband radiator and a multi-resonant wideband design.

5.1 Simulated impedance response

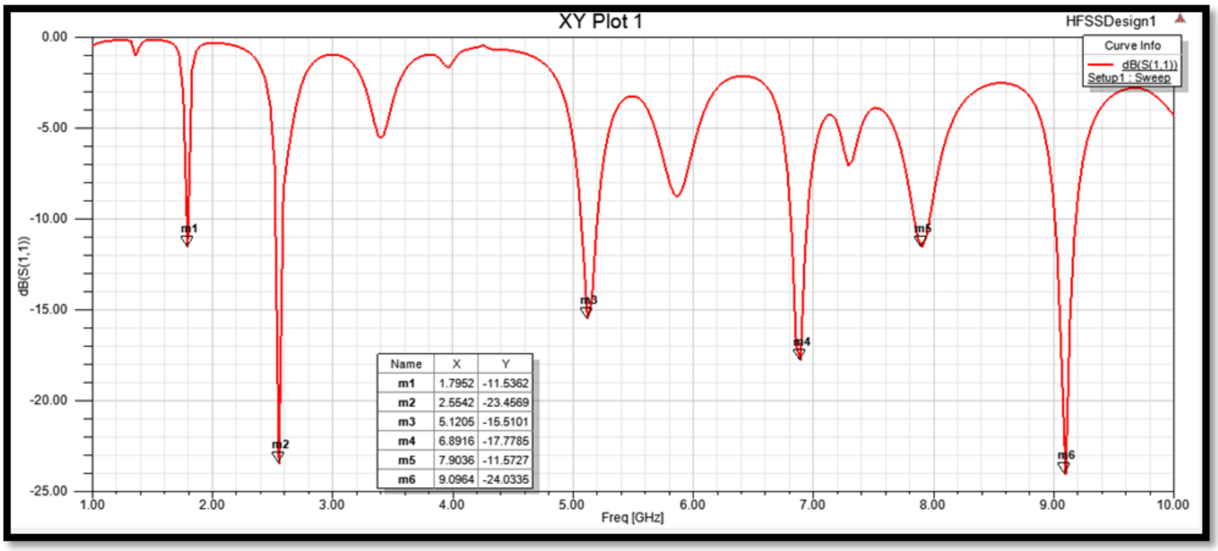

Figure 3: Simulated reflection coefficient (S11) showing six resonant minima below -10 dB.

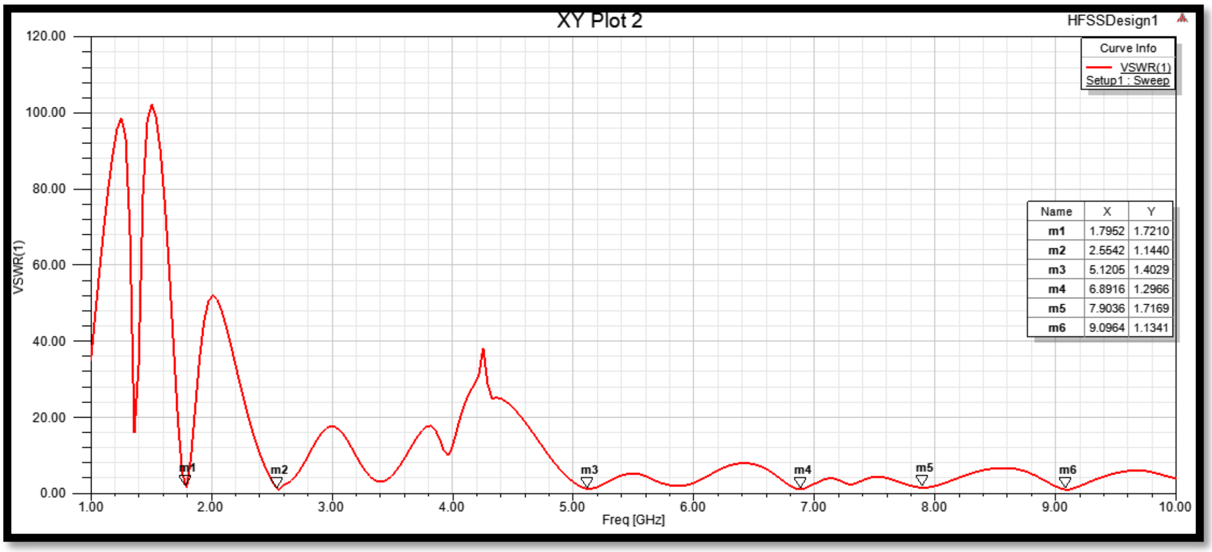

Figure 4: Simulated VSWR of the proposed antenna.

Table 2: Simulated resonant frequencies from HFSS.

Resonance no.	Frequency (GHz)	S11 (dB)	VSWR
1	1.795	-11.536	1.721
2	2.554	-23.457	1.144
3	5.120	-15.510	1.403
4	6.891	-17.779	1.297
5	7.903	-11.573	1.717
6	9.096	-24.034	1.134

The simulated return loss minima are observed at 1.795, 2.554, 5.120, 6.891, 7.903, and 9.096 GHz, with the most pronounced nulls at 2.554 GHz (-23.46 dB) and 9.06 GHz (-24.03 dB). The constructed antenna exhibits minima at 1.81, 2.62, 5.32, 6.08, 7.08, 8.24, and 9.28 GHz, with the most pronounced measured match occurring at 8.24 GHz (-30.8 dB). The supplementary resonance seen near 6.08 GHz is likely a result of fabrication-induced impacts and minor modifications in inter-arm or feed area coupling. The overall multi-resonant behavior is notably maintained post-fabrication, serving as a more robust indicator than precise point-by-point alignment.

The simulated VSWR remains below 2 throughout all six resonances, with values of 1.721, 1.144, 1.403, 1.297, 1.717, and 1.134, respectively. The annotated measured VSWR plot verifies effective matching at 2.62, 5.32, 7.08, 8.24, and 9.28 GHz, with minima approximately at 1.44, 1.34, 1.36, 1.04, and 1.40. The low recorded VSWR is at 8.24 GHz, aligning with the most pronounced return loss null observed. The assessed low frequency response is inferior to the mid and high frequency ranges, suggesting that the compact design preferentially enhances the higher order coupled modes over the fundamental resonance.

5.2 Simulated radiation and impedance behavior

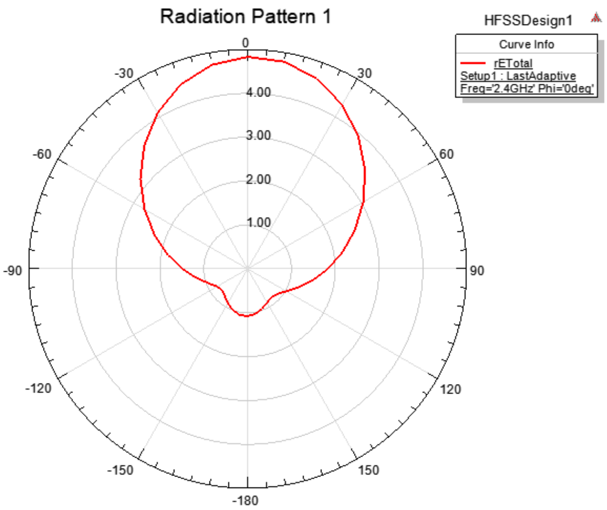

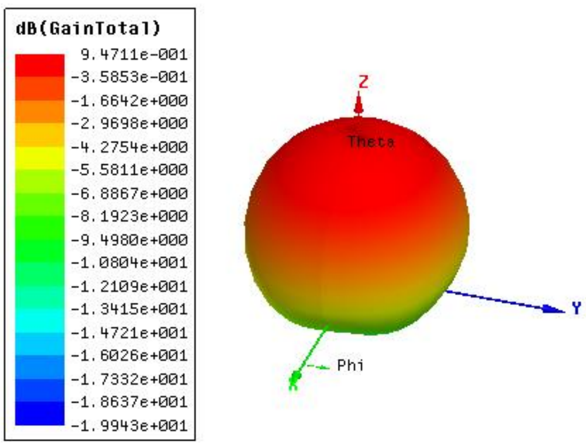

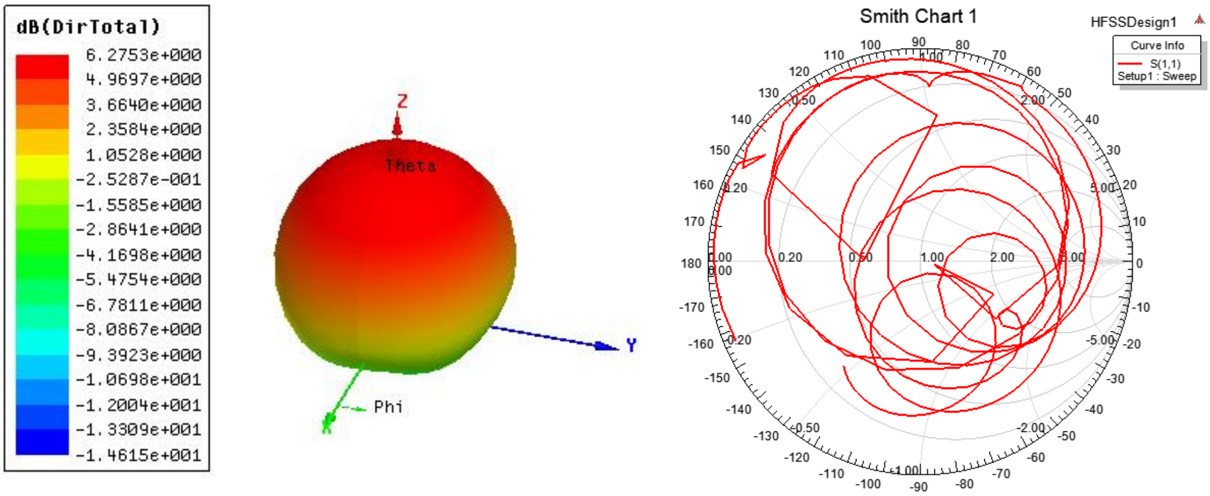

Figure 5: Simulated 2D radiation pattern, 3D related gain, 3D directivity, and Smith chart of the proposed antenna.

The simulated 2D radiation pattern reveals a predominant broadside response with minimal side-lobe degradation, whilst the 3D plots exhibit a peak directivity of around 6.275 dBi. This analytical conclusion is significant as it quantifies the penalty incurred by severe miniaturization on FR4: the antenna generates several resonant modes and achieves satisfactory matching, yet a portion of the available power is squandered instead of being radiated. The efficiency penalty elucidates why the gain remains modest despite the directivity not being exceedingly low.

The Smith chart displays several loops concentrated around the 50 Ω centers, indicative of multimode behavior. Multiple segments of the design approach the chart center, validating satisfactory impedance matching at the primary resonances. The numerous loops suggest that the extensive operating window is not attributable to a singular, straightforward resonance; instead, it arises from the convergence of several proximate resonant modes generated by various current pathways within the meander network.

5.3 Measured validation

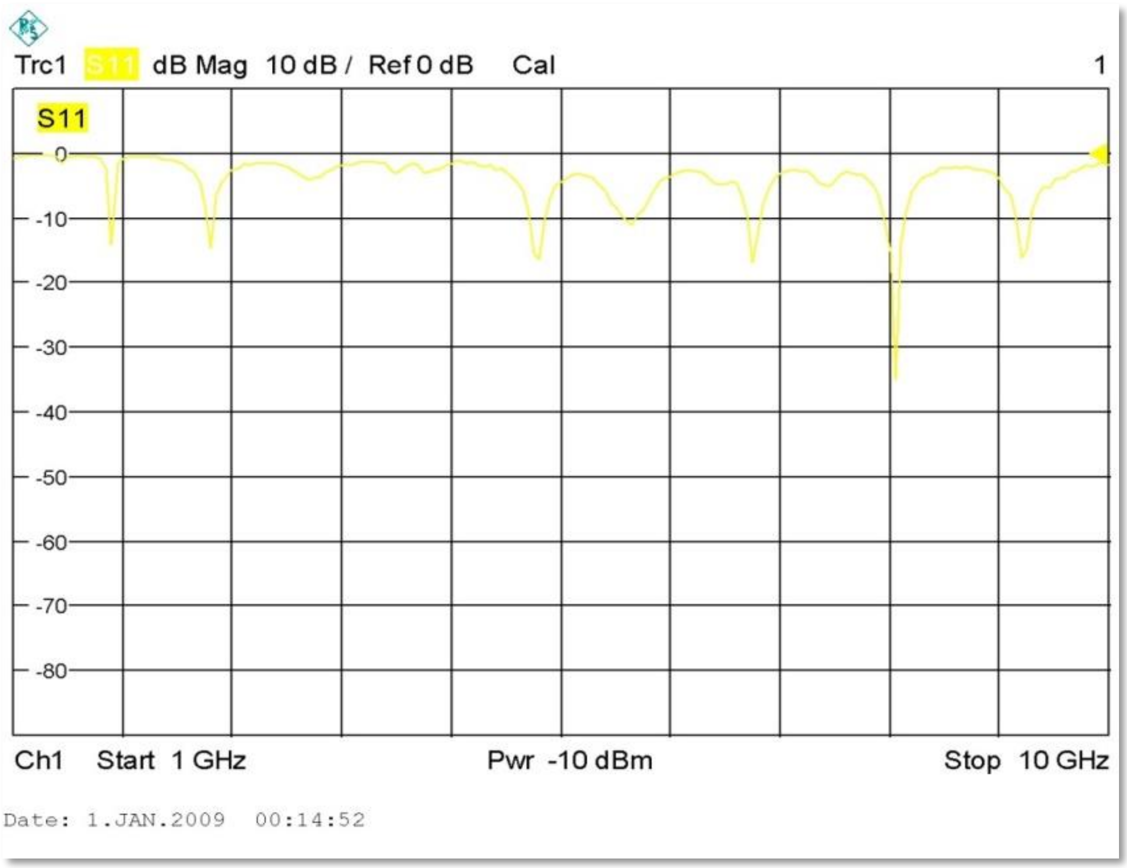

Figure 6: Measured reflection coefficient (S11) on VNA with the reported -10 dB operating window.

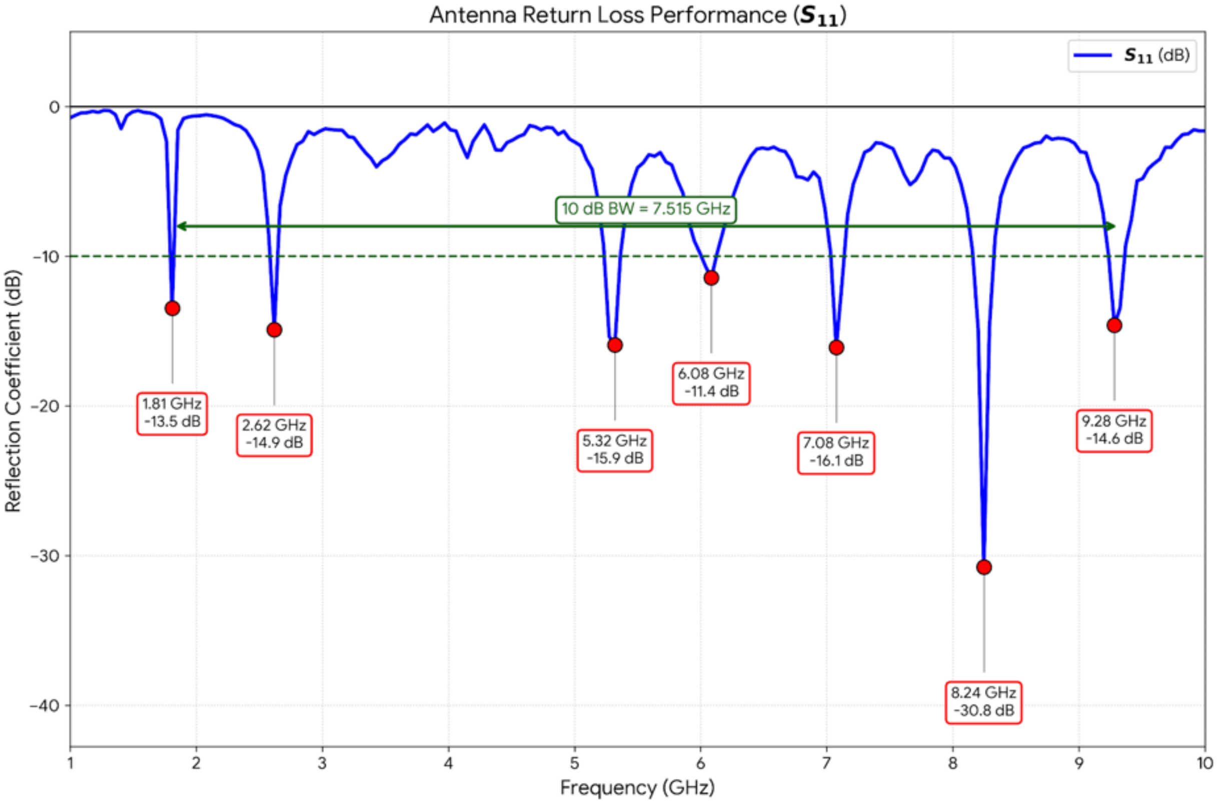

Figure 6: Measured reflection coefficient (S11) with the reported -10 dB operating window.

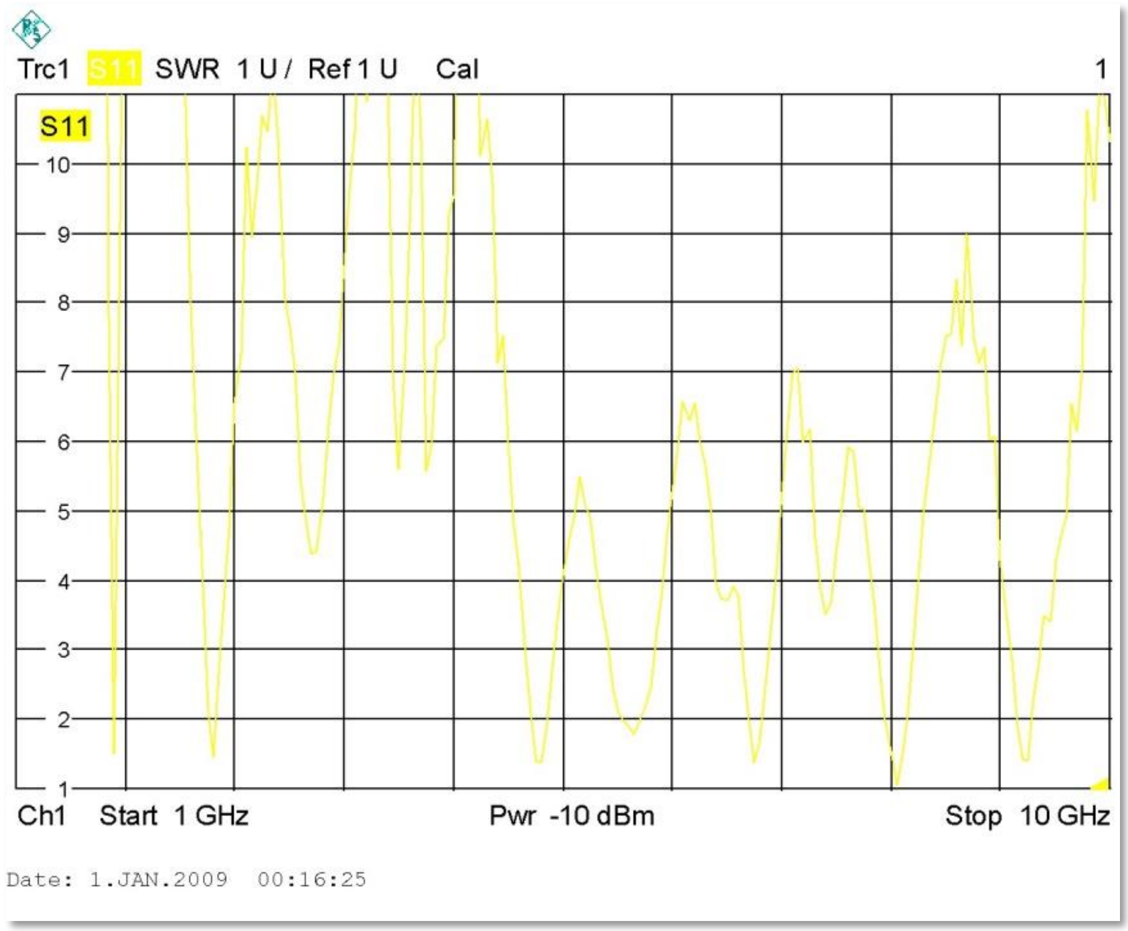

Figure 7: Measured VSWR on VNA of the fabricated antenna.

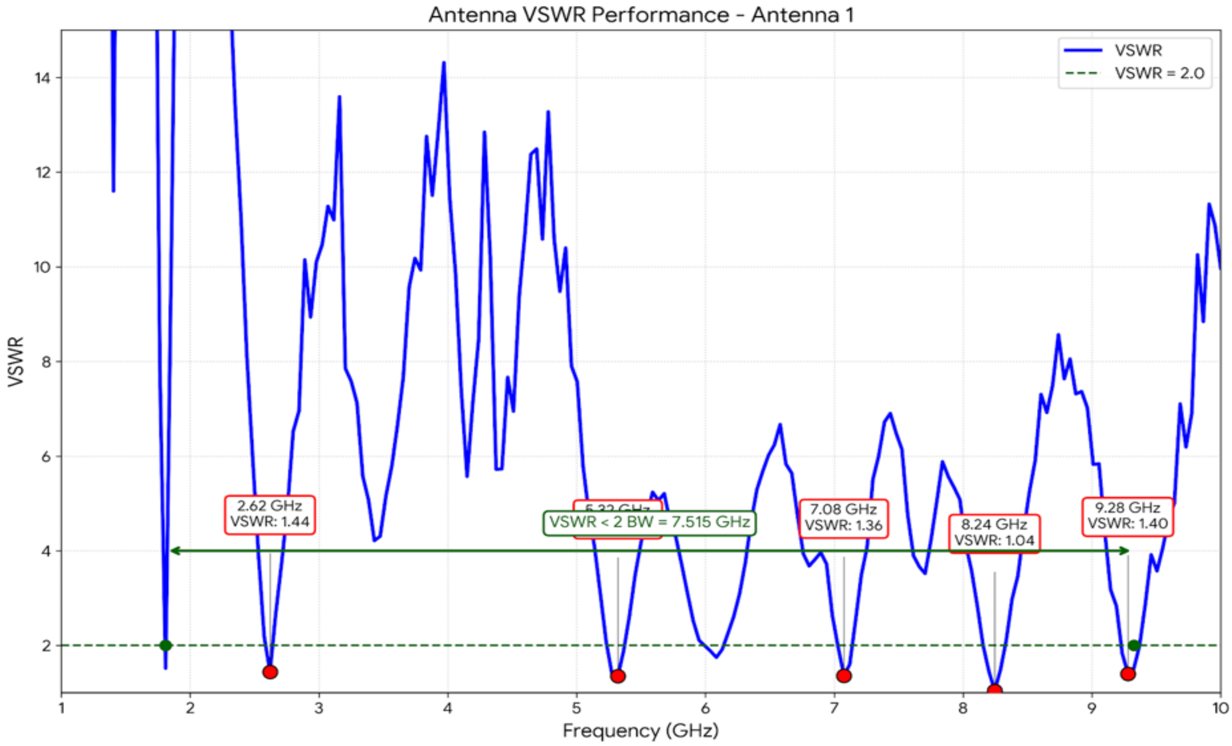

Figure 7: Measured VSWR of the fabricated antenna.

Table 3: Measured resonant frequency from the annotated plots.

Frequency (GHz)	Measured S11 (dB)	Measured VSWR
1.81	-13.5	—
2.62	-14.9	1.44
5.32	-15.9	1.34
6.08	-11.4	—
7.08	-16.1	1.36
8.24	-30.8	1.04
9.28	-14.6	1.40

The measured response retains the principal characteristics anticipated from simulation and additionally uncovers extra resonances at 6.08 GHz. The most robust measured resonance is at 8.24 GHz, with S11 = -30.8 dB and VSWR ≈ 1.04, signifying exceptional feed matching at this frequency. The measured result indicates that impedance matching is consistently acceptable across a wide high-frequency range, which is the most significant experimental feature of the design.

5.4 Simulation to measurement deviation analysis

The six directly correlated simulated and observed resonances (1.795↔1.81, 2.554↔2.62, 5.120↔5.32, 6.891↔7.08, 7.903↔8.24, and 9.096↔9.28 GHz) exhibit an average absolute frequency shift of roughly 2.73%, with a maximum shift of about 4.26%. The specified values are suitable for compact printed FR4 antennas and substantiate the assertion that the foundational design concept is empirically replicable. The additional detected mode at 6.08 GHz is more accurately understood as a fabrication-induced resonance rather than a failure of the model.

Table 4: Frequency deviation between matched simulated and measured modes.

Matched mode	Simulation (GHz)	Measurement (GHz)	Absolute shift (%)
1	1.795	1.81	0.84
2	2.554	2.62	2.58
3	5.120	5.32	3.91
4	6.891	7.08	2.74
5	7.903	8.24	4.26
6	9.096	9.28	2.02
Mean	—	—	**2.73**

5.5 Comparison with related studies

The table below indicates that the suggested antenna is competitive primarily due to its maintenance of straightforward single radiator architecture while producing a dense array of experimentally observed resonances. Its most significant comparative advantage is hence structural simplicity in relation to the number of measured modes.

Table 5: Positioning of the proposed antenna against representative compact multiband studies.

Work	Antenna Design	Reported operating behavior
Ali et al. [5] (2018)	Miniaturized slotted multiband antenna	Multiband operation
Khan et al. [7] (2019)	20×20×1.6 mm³ compact band-slot antenna	Four-band response
Patel et al. [8] (2019)	FR4 meander antenna	2.47–2.54, 4.14–4.23, 5.43–5.78, 6.71–7.42 GHz
Abolade and Konditi [10] (2021)	Compact meander + shorting pin on FR4	Six resonances
Maamria et al. [11] (2023)	Compact quad-band planar antenna with meander-line and stubs	Quad-band response
Islam et al. [4] (2023)	36 × 30 × 1.524 mm³ low-profile meander antenna	4.5, 5.0, and 5.8 GHz
Proposed Antenna	Symmetric meander micro-strip on FR4	Seven measured resonances; 7.515 GHz annotated −10 dB window

6. Limitations and future work

Although the impedance validation is convincing, the manuscript should avoid overstating its readiness for every cited wireless standard. Some measured resonances lie near, rather than exactly on, widely used bands, and the present experimental dataset is dominated by VNA-based impedance results. Since chamber-based gain, efficiency, and pattern measurements are not reported, radiation claims should remain limited to simulated behavior. The antenna as a promising compact multiresonant platform rather than as a fully finalized commercial multistandard antenna. Future work should include a measured radiation campaign in an anechoic chamber, surface-current snapshots at all resonances, tolerance analysis for SMA soldering and substrate variation, and a parametric sweep showing how arm length and inter-arm spacing control the emergence of the 6.08 and 8.24 GHz modes.

7. Conclusion

A compact multiband symmetric meandering microstrip antenna has been designed, built, and experimentally validated on a 50 × 50 × 1.6 mm³ FR4 substrate. The antenna demonstrates six simulated resonances and seven observed resonances within the frequency range of 1.8 to 9.3 GHz, supported by a verified measured -10 dB operating bandwidth of about 7.515 GHz. The mean deviation between simulation and measurement for the aligned modes is around 2.73%, indicating substantial robustness for an economical, compact printed radiator.

Simulated radiation analysis indicates that the design achieves broadside radiation with a directivity of about 6.28 dBi. The study illustrates that the physically simple symmetric meander offers an effective balance between dimensions, multi-resonant functionality, and ease of production, while indicating that further experimental radiation validation and optimization are essential for the proposed antenna.

Authors' contributions

All authors contributed equally to the conception, design, experimental work, data analysis, interpretation of results, and preparation of the manuscript. All authors reviewed and approved the final version of the manuscript for publication.

Conflicts of interest

The author declares no conflict of interest.

Funding

This research received no external funding.

Data availability

No new data were created.

References

[1] C.A. Balanis, *Antenna Theory: Analysis and Design*, 4th edn., Wiley, Hoboken, NJ (2016).
[2] K.-L. Wong, *Compact and Broadband Micro-strip Antennas*, Wiley, Hoboken, NJ (2002).
[3] J. Anguera, C. Puente, C. Borja, J. Soler, Fractal-shaped antennas: A review, *IEEE Antennas Propag. Mag.* **45** (2003) 36–46.
[4] T. Islam, M.T. Islam, R.W. Aldhaheri, M.F. Faruque, T. Alam, M.J. Singh, Low-profile meander line multiband antenna for wireless body area network (WBAN) applications with SAR analysis, *Electronics* **12** (2023) 1416.
[5] T. Ali, K.D. Prasad, R.C. Biradar, A miniaturized slotted multiband antenna for wireless applications, *J. Comput. Electron.* **17** (2018) 1056–1070.
[6] T. Ali, M.S. Aw, R.C. Biradar, A fractal quad-band antenna loaded with L-shaped slot and meta-material for wireless applications, *Int. J. Microw. Wirel. Technol.* **10** (2018) 826–834.
[7] I. Khan, T. Ali, G.D. Devanagavi, K.R. Sudhindra, R.C. Biradar, A compact multiband band slot antenna for wireless applications, *Internet Technol. Lett.* **2** (2019) e94.
[8] R. Patel, T. Upadhyaya, A. Desai, M. Palandoken, Low profile multiband meander antenna for LTE/WiMAX/WLAN and INSAT-C application, *AEU - Int. J. Electron. Commun.* **102** (2019) 90–98.
[9] R. Patel, A. Desai, T. Upadhyaya, T.K. Nguyen, H. Kaushal, V. Dhasarathan, Meandered low profile multiband antenna for wireless communication applications, *Wirel. Netw.* **27** (2021) 1–12.
[10] J.O. Abolade, D.B.O. Konditi, A shorting-pin based compact meander multiband printed monopole antenna, *Heliyon* **7** (2021) e08390.
[11] T. Maamria, M. Challal, F. Benmahmoud, K. Fertas, A. Mesloub, A novel compact quad-band planar antenna using meander-line, multi-stubs, and slots for WiMAX, WLAN, LTE/5G sub-6 GHz applications, *Int. J. Microw. Wirel. Technol.* **15** (2023) 852–859.
[12] C.-K. Lin, D.-B. Lin, H.-C. Lin, C.-C. Lin, Design of a compact multiband monopole antenna with MIMO mutual coupling reduction, *Sensors* **24** (2024) 5495.